URBAN MAPPING USING MULTITEMPORAL VERY HIGH RESOLUTION SAR DATA BY A KNOWLEDGE-BASED SEM ALGORITHM

Xin Niu[1] and Yifang Ban[2]

1. KTH Royal Institute of Technology, Division of Geoinformatics and Geodesy, Stockholm, Sweden; xin.niu@abe.kth.se
2. KTH Royal Institute of Technology , Division of Geoinformatics and Geodesy, Stockholm, Sweden; yifang@kth.se

Abstract

The objective of this research is to assess the multitemporal very high resolution single polarization SAR data for urban land cover/land-use mapping using a novel knowledge-based SEM algorithm. Three-date RADARSAT-2 ultra-fine beam SAR data were collected over the rural-urban fringe of Greater Toronto Area. A modified Stochastic Expectation-Maximization (SEM) algorithm which employs an adaptive Markov Random Field (MRF) and the Finite Mixture Model (FMM) was proposed for the supervised classification. Several SAR intensity distribution models such as Gamma, K, G0 and Fisher were compared using the algorithm. A set of rules according to the diversity of the land cover texture patterns was further applied in the decision fusion to improve the urban land cover classification. Preliminary results show that the proposed algorithm which explores the spatio-temporal information with the knowledge about the ultra-high urban SAR textures could produce reasonable classification results. Homogeneous urban land cover maps could be obtained while the detailed shape features could be preserved. Although the overall classification accuracy of the single polarization data set is not as high as desired, more details could be identified in the very high resolution SAR data. Using unique very high resolution SAR textures, rules were designed to effectively improve the classifications of several land cover classes thus improve the overall classification accuracy.

INTRODUCTION

As one of the most important remote sensing applications, urban land cover mapping has gained increasing attentions in light of the accelerating worldwide urbanizations. Within many sensors, SAR is known as an excellent observation instrument which is free from the sun-illumination and weather conditions. With the improvement of the spaceborne SAR, the urban land cover information could be extracted using very high resolution data.

Although SAR observations in high resolution have become routinely available, there is still lack of effective methods dealing for classification of multitemporal high, especially very high resolution SAR data, since higher resolution also brings higher variance within each land cover category. To this end, object-based approaches (i.e. 1, 2) are often considered as a promising way for high resolution data. However, successful employment of such approach depends on proper segmentation results which are usually difficult to achieve using the SAR data in complex urban areas. On the other hand, several pixel-based contextual approaches (i.e. 3, 4, 5, 6) have been proposed to produce homogenous mapping results with high accuracy. In (3), for example, a modified SEM algorithm employing an adaptive MRF and the FMM has been identified as an efficient approach for supervised urban mapping.

Besides the contextual information, texture information has also been used to improve urban land cover classification. Particularly, grey level co-occurrence matrix (GLCM) have long been recognized as valuable for identifying various urban patterns (i.e. 7, 8, 9), especially when using the single polarization data.

Therefore, in this paper, a novel pixel-based contextual algorithm is proposed to evaluate the multitemporal very high resolution single polarization HH data for urban mapping. Textures from the very high resolution SAR images are explored by a rule-based approach for improving the classification results. The potential and the limit of using multitemporal single polarization very high resolution SAR data for urban mapping are discussed.

METHODS

Generally, the proposed algorithm is based on a modified SEM framework as illustrated in Figure 1. Brief descriptions about each component will be given in the following subsections. For detailed information about this algorithm one could refer to (3). In this paper, further improvement is made by introducing a rule-based decision fusion process through exploring the SAR textures.

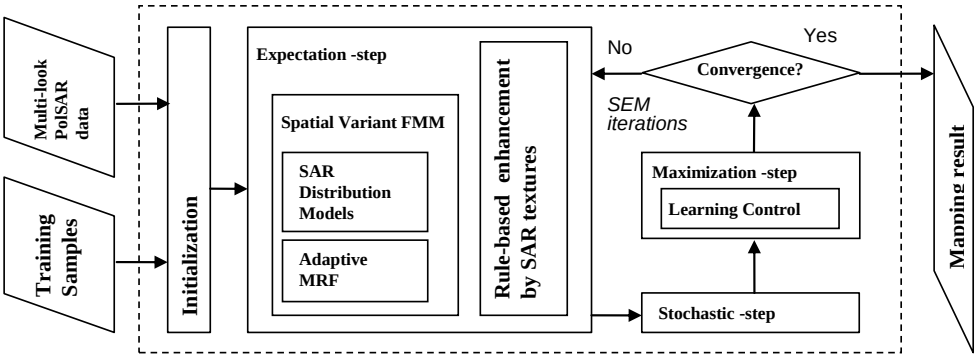

Figure 1: Flowchart of the proposed algorithm.

A. Adaptive MRF

As an effective way to explore the contextual information, MRF is often employed to model local constraints. With this assumption, the neighbourhood influence could be described by a Gibbs probability:

$$p(L_s \mid L_r, r \in \eta_s) = \frac{1}{Z_s} \exp\{-U(L_s \mid L_r, r \in \eta_s)\}. \quad [1]$$

This gives a measure of the prior probability that the pixel s is labelled as Ls when the neighbour r in the neighbourhood of s: η_s is marked as Lr. Z_s is a normalization factor. U(.) represents an energy function. Traditional MRF assumes a fixed neighbourhood structures and fixed energy function form. Such fixed configuration often leads to an "over-averaging" results and loses the structural details. To prevent such negative effects, an adaptive MRF based on an anisotropic Potts model is proposed by adaptively selected the neighbourhood shapes and the impact of the MRF analysis. The best neighbourhood shape which is assumed to have the lowest standard deviation will be selected from the five candidate templates as illustrated in Figure 2.

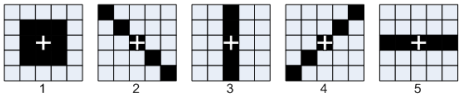

Figure 2: Candidate neighbourhoods for adaptive MRF.

Moreover, an adaptive energy function is given as:

$$U(L_s \mid L_r, r \in \eta_s) = -(\beta(1-b_s)\sum_{r \in \eta_s} \delta(L_s - L_r)). \quad [2]$$

where β is the Ising-Potts model impact. $\delta(\cdot)$ is the Kronecker delta function. bs measures the homogeneity of the neighborhood η_s . The calculation of bs could be found in (10).

B. Spatial Variant FMM

FMM is commonly used to represent the heterogeneity of the observations. FMM assumes each datum is a mixture of a finite number of latent classes. The weight of each class is measured by the normalized probabilities. By FMM, the Probability Density Function (PDF) of an intensity observation I at location s is expressed as:

$$f(C_s) = \sum_{i=1}^{g} \rho_i f_i(I_s \mid \Theta) \quad [3]$$

where ρ_i is the prior probability of class i in g classes. According to the spatially variant FMM (11), it could also be represented by the MRF prior probability. $f_i(I_s \mid \Theta)$ is the likelihood of the intensity observation for class i with the model parameters denoted by Θ. For simplicity, the likelihood of multitemporal observations was modelled as the product of the PDFs from each date intensity data. Therefore, the mixture model density function could be rewritten as:

$$f(C_s) = \sum_{i=1}^{g} \rho_{si} f_i(I_s \mid \Theta) = \sum_{i=1}^{g} p(L_s = i \mid L_r, r \in \eta_s)(\prod_{t=1}^{m} f_{it}(I_{st} \mid \theta_{it})) \quad [4]$$

Where $f_{it}(I_{st} \mid \theta_{it})$ is the PDF of the intensity distribution of class i on date t. θ_{it} are the corresponding distribution parameters. I_{st} is the observation of the date t. m is the total dates.

C. Contextual SEM

To estimate the distribution models in the clustering process, SEM algorithm is often employed. Indicating the iteration index by the superscript k, the proposed contextual algorithm could be described as follow:

Initialization: estimating the initial intensity distribution parameter θ_{it}^0 of each class in each date according to the training samples. The initial MRF prior probability is equally set with 1.

E (Expectation)-Step: for each pixel s, calculate the MRF probability $p^k(L_s \mid L_r, r \in \eta_s)$ based on the classification of the last iteration and update the posterior probabilities for each class i by

$$\tau_{si}^k = \frac{p^k(L_s = i \mid L_r, r \in \eta_s)(\prod_{t=1}^{m} f_{it}(C_{st} \mid \theta_{it}^k))}{\sum_{l=1}^{g} p^k(L_s = l \mid L_r, r \in \eta_s)(\prod_{t=1}^{m} f_{lt}(C_{st} \mid \theta_{lt}^k))} \quad [5]$$

S (Stochastic)-Step: according to the posterior probability τ_{si}^k, randomly label the current pixel. After all the pixels, a new map is generated with the pixels classified into g class $\{Q_1^k, \cdots, Q_g^k\}$.

M (Maximization)-Step: update the intensity distribution parameters θ_{it}^{k+1} with the pixels belonging to the class group Q_i^k for each date.

Such E-, S- and M- steps form an iteration cycle, and runs until the convergence point is met. To prevent the degenerate problems, a learning control scheme based on the similarity measure is further provided in the M-Step. Details about such algorithm could be found in (3).

D. Texture Enhancement Scheme

Through analysing the GLCM textures of the very high resolution SAR data, we have found there is obvious difference between the urban and non-urban area by using the GLCM 2nd moment parameters. And the GLCM dissimilarity could be an efficient indicator for distinguishing the low-density (LD) and high-density (HD) areas. Such GLCM texture differences for identifying the urban patterns from the very high resolution data are found even more significant than that from the high resolution data. Moreover, the temporal characteristics of the GLCM textures are noticed for classifying the forest and crops. For example, the GLCM 2nd moment of Jun. 25 SAR is better to differentiate the forest and crop2. And the GLCM Mean ratio of Sep. 02 to Jun. 25 SAR is useful to separate the forest and crop1. Based on such knowledge, a texture enhancement scheme is proposed as illustrated in Figure 3.

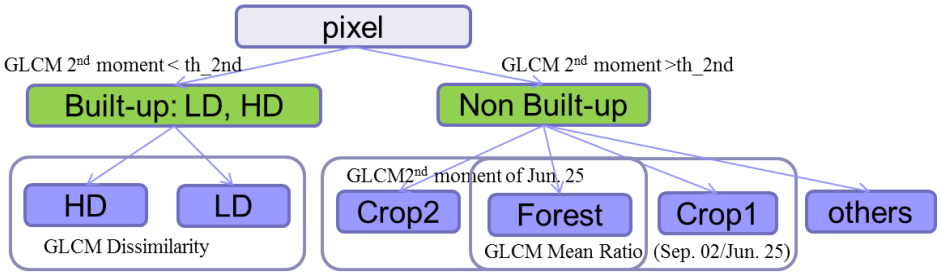

Figure 3: Texture enhancement scheme.

First, each pixel is assigned to the built-up and non-built-up areas. For the built-up area, the FMM only includes the LD, HD classes. For the non-built-up area, the other classes are counted in. Therefore, the latent finite class group is g={built-up classes} or {non built-up classes} in the above mentioned situations. The texture based decision is fused with the posterior probabilities [5]. For the two classes which could be further differentiated by certain texture information, i prefers the smaller texture value, but j prefers the higher texture value, the new posterior probabilities are given as:

$$\begin{cases} \tau_{si}^{k}\_with\_texture = \tau_{si}^{k} \cdot (th\_ij / val\_texture) \\ \tau_{sj}^{k}\_with\_texture = \tau_{sj}^{k} \cdot (val\_texture / th\_ij) \end{cases} \quad [6]$$

DATA AND EXPERIMENTS

Three-dates RADARSAT-2 ultra-fine beam C-HH SAR data with the nominal pixel spacing about three meters were collected over the rural-urban fringe of Greater Toronto Area in Jun. 25, Aug. 12 and Sep. 05, 2008. They are all in ascending orbit with similar incident angles (30.6-32.0°). The images are first orthorectified and then followed by a multi-look process with a 4x4 window. The pixel spacing of the final prepared images is 8 x 8 meters. The major land cover classes were high-density built-up areas (HD), low-density built-up areas (LD), grass, golf course, forest, water and two types of crops. Training samples for each class is about 1600. Test samples were randomly selected. Four common intensity distribution models, namely Gamma, K, G0 and Fisher (12, 13) were compared in the proposed algorithm which is further optimized with parallel computing in C++.

RESULTS AND DISSCUSSION

The very high resolution multitemporal data was evaluated first without the texture enhancement rules (Table 1). It was found that the overall classification accuracies for all models are rather poor. Over all, G0 and Fisher could produce better results than K and Gamma models with comparable time cost. K model cost considerable longer time. G0 and Fisher all had better performance for the built-up areas as LD and HD. Water, grass and crop 2 achieve good classification results for all models. However, for any model, the producer accuracy of LD is near 0, which could also be observed in the selected result samples by the G0 model in Figure 4.

By applying the texture enhancement rules, significant improvement could be observed as summarized in Table 1 and compared in Figure 4. Such enhancement is more evident for the LD class, Forest and crops, as the rules were designed for. Using the texture rules, almost all the LD area could be correctly identified, which also improved the user accuracy of the Forest. By the rules for distinguishing forest and crops, the producer accuracy of forest and user accuracy of crops also increased significantly. The texture strategy also improves the HD class as well. The overall accuracy and Kappa were improved significantly. Moreover, such improvement only cost very little extra time considering the total time is from 15.7 min without rules to 17.1 min with rules.

Table 1: Results using various intensity distribution models and improvement by the rules. “P” and “U” are respectively the producer and user accuracy. OA is overall accuracy.

	Gamma		K		G0		Fisher		G0+rules	
	P	U	P	U	P	U	P	U	P	U
Water	0.87	0.81	0.88	0.82	0.87	0.85	0.87	0.84	0.87	0.85
Golf course	0.52	0.55	0.54	0.56	0.63	0.57	0.62	0.55	0.63	0.57
Grass	0.78	0.69	0.76	0.68	0.75	0.69	0.74	0.68	0.65	0.72
LD	0.01	0.31	0.01	0.32	0.07	0.49	0.05	0.46	0.92	0.72
Crop1	0.72	0.48	0.71	0.47	0.69	0.46	0.71	0.47	0.68	0.66
Crop2	0.88	0.53	0.87	0.53	0.87	0.62	0.86	0.60	0.89	0.90
Forest	0.50	0.27	0.51	0.27	0.52	0.33	0.52	0.31	0.78	0.63
HD	0.47	0.83	0.48	0.83	0.62	0.76	0.60	0.78	0.67	0.94
OA	0.54		0.54		0.59		0.58		0.77	
Kappa	0.46		0.46		0.51		0.50		0.73	
Average Iteration time	2.1 min		3.3 min		2.2 min		2.2 min		2.4 min	
Total time	14.5 min		23.3 min		15.7 min		15.8 min		17.1 min	

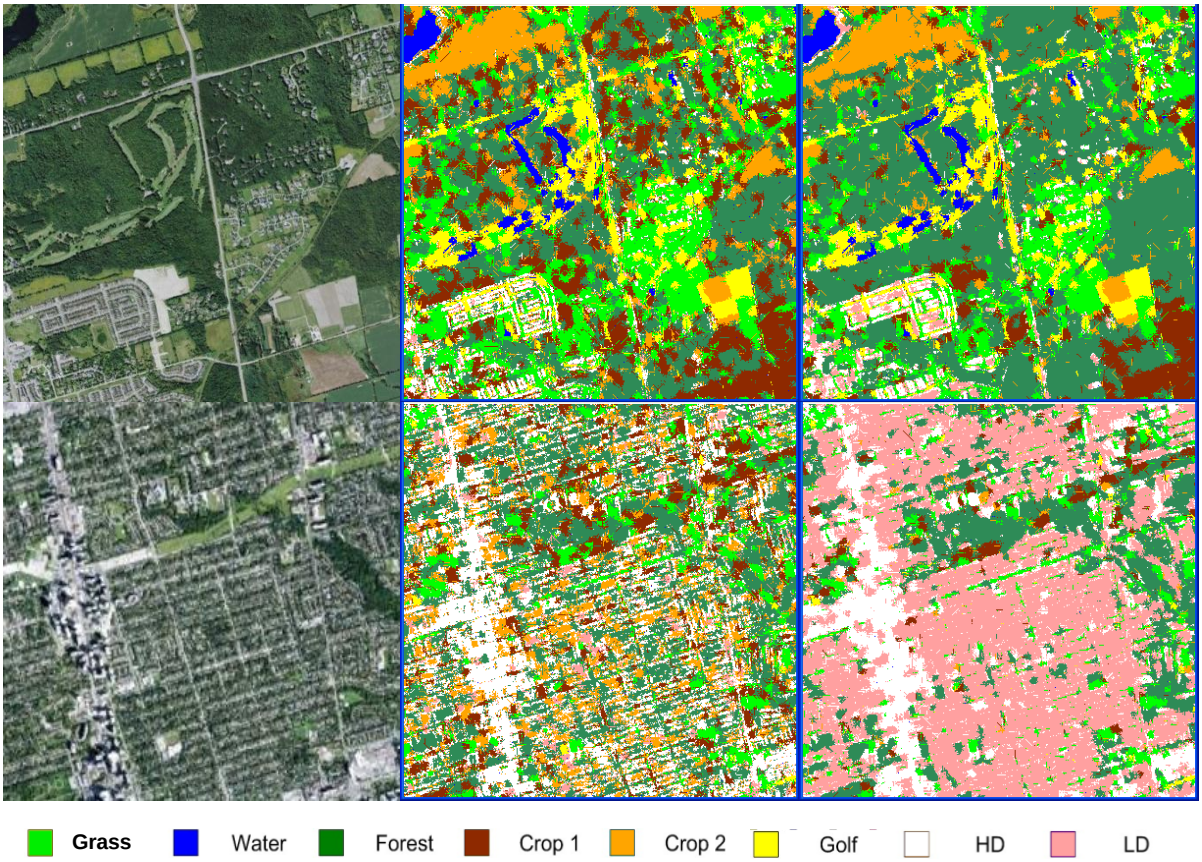

Figure 4: Selected samples of the classification results. Left column: ground truth; Middle column: using G0 model without texture rules; Right column: using G0 model with texture rules.

CONCLUSION

The proposed Knowledge-Based SEM Algorithm could integrate the spatio-temporal information to produce homogenous mapping results with reasonable accuracy. Texture information could be effectively explored by the rules to significantly enhance the results with small time cost. Although very high resolution single polarization HH SAR data has limited ability for urban mapping, the unique very high resolution textures have the great potential to improve urban land cover classification.

ACKNOWLEDGEMENTS

The authors thank the Swedish National Space Board for funding this research and the Canadian Space Agency for providing the RADARSAT-2 polarimetric SAR data.

References

1 Ban Y, H Hu and I M Rangel, 2010, Fusion of QuickBird MS and RADARSAT SAR data for urban land-cover mapping: object-based and knowledge-based approach. International Journal Remote Sensing, 31: 1391-1410.

2 Niu X and Y Ban, 2012, Multitemporal RADARSAT-2 Polarimetric SAR Data for Urban Land Cover Classification using an Object-based Support Vector Machine and a Rule-based Approach. International Journal of Remote Sensing, accepted for publication.

3 Niu X and Y Ban, 2012, An adaptive contextual SEM algorithm for urban land cover mapping using multitemporal high-resolution polarimetric SAR data. IEEE Journal of Selected Topics in Applied Earth Observations and Remote Sensing, accepted for publication.

4 Zhong P and R Wang, 2009, Image segmentation based on Markov random fields with adaptive neighborhood systems. Optical Engineering, 45: 462-465.

5 Garzelli A, 1999, Classification of polarimetric SAR images using adaptive neighborhood structures. International Journal of Remote Sensing, 20: 1669-1675.

6 Wu Y, K. Ji, W. Yu and Y. Su, 2008, Region-based classification of polarimetric SAR images using Wishart MRF. IEEE Geoscience and Remote Sensing Letters, 5: 668-672.

7 Ban. Y. and Q. Wu. 2005. “RADARSAT fine-beam SAR and GIS data for urban Landuse and land-cover mapping“, In: Proceedings, 8th AGILE Conference on GIScience, Estoril, Portugal.

8 Gamba P, M Aldrighi and M Stasolla, 2011, Robust Extraction of Urban Area Extents in HR and VHR SAR Images. IEEE Journal of Selected Topics in Applied Earth Observations and Remote Sensing, 4: 27-34.

9 Dell'Acqua F and P Gamba, 2003, Texture-based characterization of urban environments on satellite SAR images. IEEE Transactions on Geoscience and Remote Sensing, 41: 153-159.

10 Lee Jong-Sen, MR Grunes and G de Grandi, 1999, Polarimetric SAR speckle filtering and its implication for classification. IEEE Transactions on Geoscience and Remote Sensing, 37: 2363-2373.

11 Celeux G, F Forbes, and N Peyrard, 2003, EM procedures using mean field-like approximations for Markov model-based image segmentation. Pattern Recognition, 36: 131–144.

12 Tison C, J-M Nicolas, F Tupin, and H Maître, 2004, A new statistical model for Markovian classification of urban areas in high-resolution SAR images. IEEE Transactions on Geoscience and Remote Sensing, 42: 2046–2057.

13 Frery A C, H-J Muller, C C F Yanasse, and S J S Sant'Anna, 1997, A model for extremely heterogeneous clutter. IEEE Transactions on Geoscience and Remote Sensing, 35: 648-659.